3D Carbon Nanotube Architectures on Glass Substrate by Stamp Printing Bimetallic Fe−Pt/Polymer Catalyst

Shaoming Huang* and Albert W. H. Mau

CSIRO Molecular Science, Bag 10, Clayton South, Victoria 3169, Australia

Received: March 18, 2003; In Final Form: June 13, 2003

We described a simple and feasible method for controlled fabrication of 3D carbon nanotube (CNT) architectures on glass at low temperatures (550−650 °C) on a large scale by stamp printing bimetallic Fe−Pt/polymer catalyst onto the substrate. The incorporation of Pt into the Fe catalyst was found to greatly decrease the growth temperature of the CNTs. By controlling the concentration of the catalyst and the stamp printing condition, 3D CNT architectures can be achieved. The formation mechanism of these 3D architectures and the function of Pt in the catalytic growth of CNTs are also discussed.

Patterning two-dimensional aligned/nonaligned carbon nanotubes (CNTs) on substrates for device applications has been demonstrated using various techniques including offset printing,[1] standard lithography,[2−4] soft lithography,[5−7] and self-assembly.[8] Some attention has been paid to 3D CNT patterning recently.[9,10] 3D architectures of CNTs could be useful for developing new nanotube-based devices and some of the applications. For example, using patterned 3D architectures of CNTs as an electron emission source, one can expect that electron can emit from nanotubes located at different regions at different voltages or the electron density could be different at a different pattern region. For practical applications, controlled fabrication of CNTs at low temperature is strongly desired (lower than 666 °C so that glass can be used as substrate; the strain point of the best display glass is 666 °C). Many efforts have been made to synthesize CNTs at low temperatures using various techniques, such as the plasma-enhanced CVD technique.[11−13] However, controlled fabrication of multidimensional, particularly 3D, CNT patterns in large areas and at low temperatures is still a challenge. Most recently, we have developed a method to photolithographically pattern aligned carbon nanotubes/nanofibers directly on the substrate using CVD by incorporating a catalyst precursor into the polymer photoresist.[14] However, the temperature is still a critical issue for CNT growth. It was found that when the temperature is lower than 700 °C, carbon nanofibers rather than nanotubes are normally obtained, which is also observed by many other researchers. In this paper we described a simple and feasible method for controlled fabrication of 3D CNT architectures on glass at low temperatures (550−650 °C) on a large scale by stamp printing bimetallic Fe−Pt/polymer catalyst onto the substrate. The incorporation of Pt into the Fe catalyst was found to greatly decrease the growth temperature of the CNTs. By controlling the concentration of the catalyst and the stamp printing condition, 3D CNT architectures can be achieved. The general procedure is outlined in Scheme 1. It involves stamp printing mixed inorganic salt-containing polymer solution on a glass substrate followed by an oxidation process to remove the polymer matrix and a reduction process to produce nanosized metal catalysts for CNT growth by pyrolysis of acetylene at 550−650 °C. The formation mechanism of these 3D architectures and the function of Pt in the catalytic growth of CNTs are also discussed.

SCHEME 1: Schematic Illustration of the Procedure for the Growth of Three-Dimensional CNT Architectures Based on CVD by Stamp Printing a Catalyst Precursor-Containing Polymer Solution on a Glass Substrate

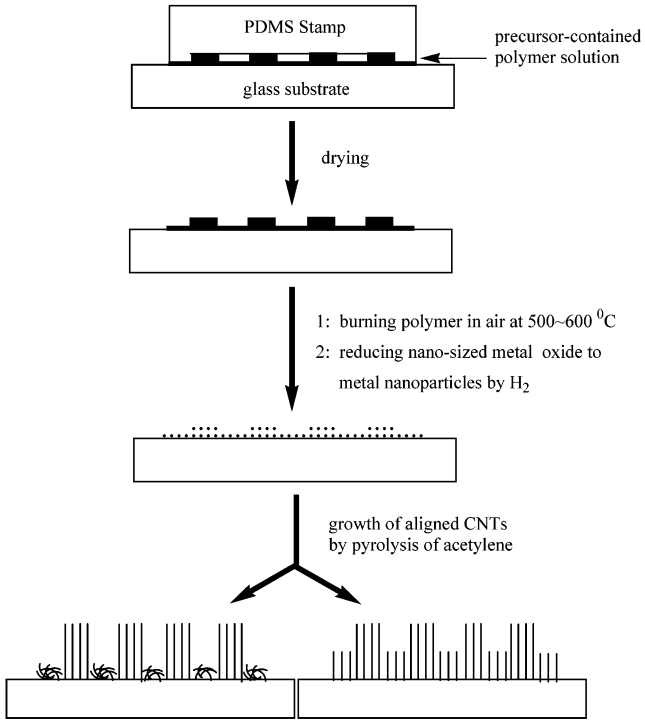

In a typical experiment, a drop of an aqueous solution of water-soluble polymer (PVA, MW = 89 000) containing Fe-$(NO_3)_3 6H_2O$ and H_2PtCl_6) (concentration of iron, 50−400 mM; mole ratio of Fe/Pt, 3−5/1; and polymer wt %, 3−5%) was placed on the glass substrate (Corning glass). Patterned PDMS stamps were prepared from Sylgard 184 (Dow Corning, Midland, MI) on masters (prepared by photolithography). The stamp was then put on the substrate with a certain pressure and dried at 120 °C for 30−60 min. After the stamp was released, the substrate with polymer patterns was heated in air at the rate

* Present address: Chemistry Department, Duke University, Durham, NC 27708. E-mail: smhuang@duke.edu.

10.1021/jp034705+ CCC: $25.00
Published on Web 07/18/2003

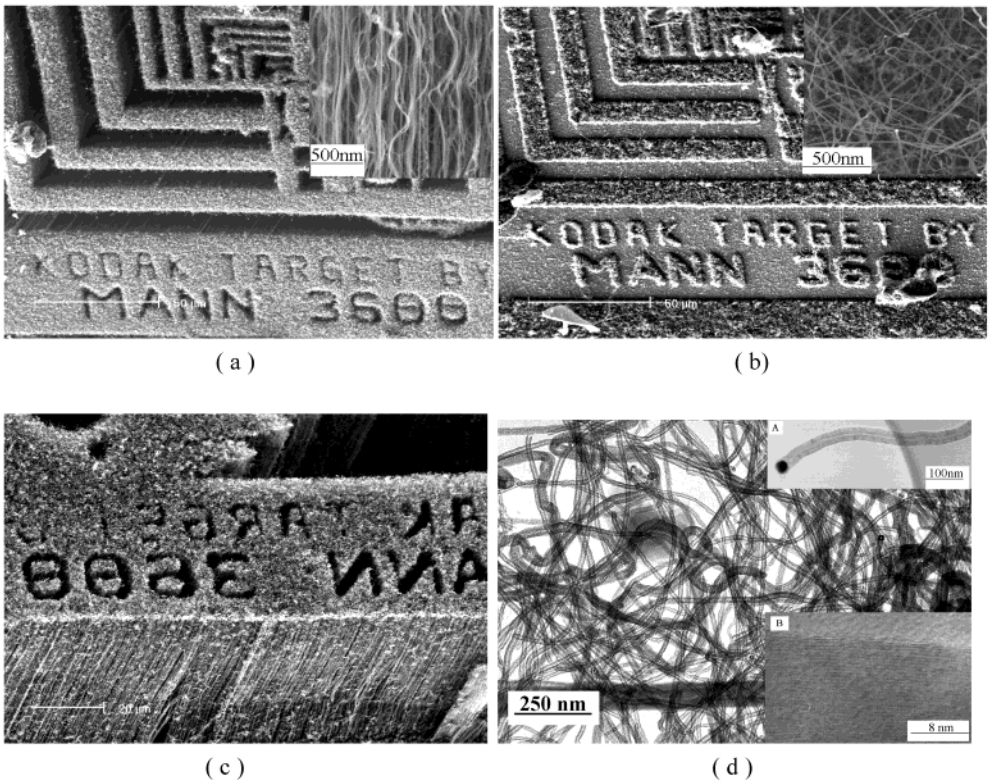

Figure 1. SEM images of 3D CNT architecture on a glass substrate generated by pyrolysis of acetylene at 650 °C for 60 min by stamp printing bimetallic Fe/Pt catalyst (Fe^{3+}, 200 mM; Pt^{4+}, 50 mM; PVA, 4 wt %). (a) Low magnification of the pattern. Inset a is the high-magnification image showing densely packed aligned CNTs. (b) Converted pattern after removal of the aligned CNT pattern. The inset is the high-magnification image showing the random entangled CNTs. (c) Turned-over pattern keeping the original pattern structure. (d) TEM image of the generated CNTs. Inset A shows the hollow structure and the catalyst particle on the tip of the individual nanotube, and inset B shows the HRTEM of nanotube with graphitized layer structure.

of 20 °C/min up to 500−600 °C in a conventional tube furnace and kept for 1−2 h. During this oxidation process the metal salt precursors became nanosized metal oxide particles located on the patterned regions and the polymer matrix was decomposed. Then, the nanosized metal oxide particles were reduced by H_2/Ar at 500−600 °C for 1−2 h to form metallic nanoparticles. Acetylene/Ar was then introduced (V:V, 1:3; total flow rate 40−80 mL/min) at 550−650 °C for times ranging from a few minutes to 1 h to grow 3D aligned CNT patterns. The samples were characterized by scanning electron microscopy (SEM, XL-30 FEG SEM, Philips, 5 kV), transmission electron microscopy, and high-resolution electron microscopy (TEM and HRTEM, JEOL 2010, 300 kV).

Figure 1a shows the typical scanning electron microscopic (SEM) images of aligned CNT patterns produced by pyrolysis of acetylene at 650 °C for 60 min after stamp printing $Fe(NO_3)_3-H_2PtCl_2$/PVA (poly(vinyl alcohol)) aqueous solution (Fe^{3+}, 200 mM; Pt^{4+}, 50 mM; PVA, 4 wt %) on glass substrates (Corning glass). The high magnification of the SEM image (inset 1a) shows that the as-synthesized CNTs are straight and densely packed. The length of the aligned CNTs was measured to be ca. 40 μm with a very uniform diameter in the 20−40 nm range. The resolution of the pattern can be as small as submicron scale. It was very interesting to find that after removing the longer aligned CNT pattern from the substrate with adhesive tape, the remaining pattern (the "converted" pattern) can be easily seen on the substrate (Figure 1b). A high-magnification SEM image shows that they are random entangled CNTs (inset 1b). The removed, patterned CNTs still keep their original structure, as shown in Figure 1c. In this 3D CNT architectures, the removed pattern is an aligned CNT array and the converted pattern is random. Transmission electron microscopy (TEM and HRTEM) observations clearly indicate that these CNTs are multiwall nanotubes with well-graphitized structure rather than nanofibers (Figure 1d). The hollow structure and the catalyst particle at the tip of an individual nanotube can be seen in inset A in Figure 1d and the well-graphitized structure is shown in inset B. The formation of these 3D architectures was believed to be mainly due to the different density of the catalyst on the different pattern areas. Detailed SEM observations show that Fe_2O_3/PtO_2 nanoparticles in the range of 10−50 nm in diameter are formed after decomposing the polymer matrix at 550 °C in air. It was also found that the density of catalyst in the pattern area (white region in Figure 2, shown in inset 2a) is higher than that in the converted pattern region (dark region in Figure 2, shown in inset 2b). This result indicates that the alignment of the CNTs depends strongly on the density of the catalyst on the substrate. A higher density of catalyst will help the alignment of CNTs. In our case, when the concentration of Fe^{3+} is lower than 100 mM, only random entangled CNTs are formed on the pattern regions. In case of the low density of catalyst, CNTs have a large volume where they can grow, which results in a highly random entangled film, as shown in the high-magnification SEM image (inset in Figure 1b). The situation is different in the case of high catalyst density. van der Waals interactions with neighboring CNTs force the CNTs to only grow normal to the substrate. As they lengthen, neighboring CNTs form bundles. From the SEM image (Figure 1a) it can be clearly seen that the interactions between CNTs are so strong that even the outermost CNTs are held together without branching away. The average space between nanotubes is estimated to be 10−20 nm, which is roughly consistent with the density of catalyst nanoparticles. The density of the aligned CNTs is so high that we can actually transfer the pattern (turned-over pattern) by adhesive tape from the glass substrate without

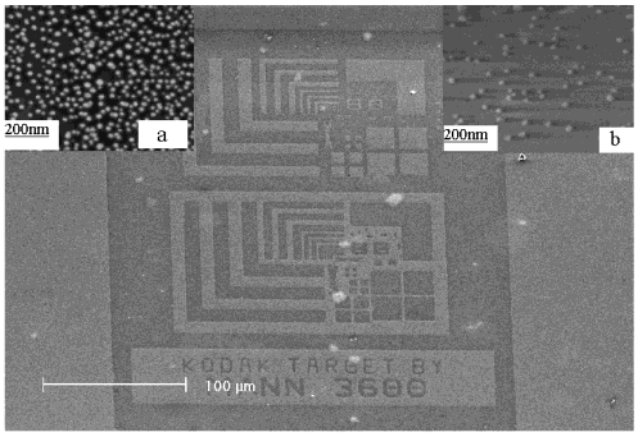

Figure 2. SEM image of low magnification of the pattern on a glass substrate by stamp printing $Fe(NO_3)_3 6H_2O/H_2PtCl_6$)/PVA aqueous solution ($Fe^{3+}$, 200 mM; Pt^{4+}, 50 mM; PVA, 4 wt %) followed by oxidation treatment at 550 °C for 2 h. Insets a and b are the high-magnification SEM images of the pattern area (white region) and converted pattern area (black region), respectively.

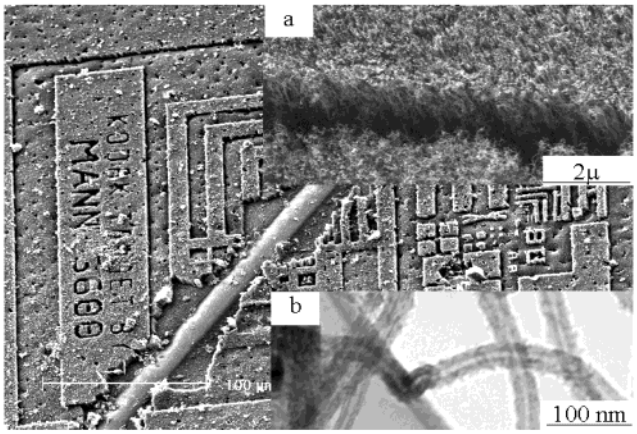

Figure 3. SEM image of large-area 3D CNT patterns on glass substrates generated by pyrolysis of acetylene at 550 °C for 20 min by stamp printing bimetallic Fe/Pt catalyst (Fe^{3+}, 300 mM; Pt^{4+}, 75 mM; PVA, 4 wt %). Insets a and b are the high-magnification SEM image of the pattern and the TEM image of an individual nanotube, respectively.

destroying its structure.(Figure 1c). This enables us to be able to transfer the pattern to other substrates, e.g., plastics, which are not suitable for direct growth at high temperature, conducting substrates such as metals and other materials such as ceramics.

The structure of the 3D CNT architecture can be controlled by changing the concentration of catalyst and also controlling the pressure put onto the stamp during stamp printing. Increasing the concentration of catalyst or decreasing the pressure creates a higher density of the catalyst on the pattern region and the converted pattern regions as well, as described in Scheme 1. Aligned CNTs could grow on both pattern areas when the density of the catalyst on both regions was high enough. Figure 3a is the typical SEM image of a large area 3D CNT architecture produced by pyrolysis of acetylene at 550 °C for 20 min by using the same polymer solution as above but with high concentration of catalyst (Fe^{3+}, 300 mM; Pt^{4+}, 75 mM; PVA wt %, 4%). After scratching the surface, it is easy to observe the 3D architectures of both aligned CNT patterns. Insert 3a is a high-magnification SEM image showing the different lengths of the aligned CNTs on different pattern regions. TEM observation confirmed the CNT structure shown in insert 3b. The pattern with longer aligned CNTs (ca. 8 μm) is the high-density-catalyst area and the converted pattern has shorter CNT length (ca. 5 μm). Although the converted pattern region has less catalyst density, the concentration is still high enough for growth of aligned CNTs. The reason for the different lengths of the nanotubes in different patterns is still not fully understood at this stage. It is thought to be due to the different growth rate of CNTs at different areas and also to the nonuniform concentration of acetylene in the local regions. Because the adsorption and decomposition of acetylene molecules onto the surface of the Fe/Pt catalyst is an exothermic process, the local temperature at the area of high-density catalyst in the initial stages of nucleation will be higher, which will result in a faster growth rate of CNTs in this area. On the other hand, in the high-density-catalyst area the consumption of acetylene molecules will be greater. Acetylene molecules will diffuse from areas where the density of the catalyst is lower and the consumption of acetylene is less, resulting in the nonuniform concentration of acetylene in local regions.

The growth and structure of CNTs strongly depends on the temperature. Our experimental results showed that CNTs can only be generated at temperatures over 700 °C by pyrolysis of acetylene using Fe catalyst (using $Fe(NO_3)_3$ as precursor).[14] It is known that Pt nanoparticles are not active for the CNT growth.[15] However, when Fe−Pt bimetallic catalyst was used, the growth temperature of CNTs can be decreased to 550 °C. Early studies by Baker[16] showed that carbon filaments (actually carbon nanotubes) can form by pyrolyzing acetylene at 417 °C over bimetallic Pt/Fe catalyst prepared by thermally evaporating Pt/Fe alloy wire on a substrate followed by thermal treatment under hydrogen or argon. Sequential impregnation or coimpregnation of iron salt (e.g., $FeCl_3$, $Fe(NO_3)_3$) and platinum salts (e.g., H_2PtCl_6, K_2PtCl_6 or $Pt(NH_3)_4(OH)_2$) on porous supports such as SiO_2, Al_2O_3) followed by H_2 reduction is a common way to prepare bimetallic Fe/Pt supported catalysts.[17−19] and the reduction process at high temperature normally results in the formation of α- or γ-Fe/Pt solid solution nanoparticles.[17] So it is believed that in our case the similar situation could exist, i.e., the formation of bimetallic Fe/Pt nanoparticles. It is known that the adsorption and decomposition of acetylene on Pt surfaces is much easier than on Fe surfaces. This process is highly exothermic, 53.5 kcal/mol. So, it is possible that in the case of Fe/Pt nanoparticles, the decomposition of acetylene occurs initially on the exposed Pt surface and the large amount of heating due to the decomposition makes the local temperature significantly higher than the furnace set temperature. Then the carbon will tend to move toward the adjacent Fe surface for nanotube growth, although the detailed structure of the bimetallic Fe/Pt catalysts and the influences of the concentration of the precursors on the composition and structures of the bimetallic nanoparticles are not clear at this stage. Using this rationale, it is understandable that the growth rate of CNTs in the high-density-catalyst region would be higher. The incorporation of Pt into Fe catalyst greatly decreases the growth temperature of CNTs, which makes this catalyst system advantageous for generating aligned CNTs on glass substrates for device fabrication and applications.

In summary, we have presented a simple and feasible method to fabricate three-dimensional CNT architectures on a substrate on a large scale by stamp printing inorganic salt-containing polymer solutions followed by oxidation and reduction procedures and pyrolysis of acetylene. Using bimetallic Fe/Pt catalyst, CNTs can be generated at low temperature (550−650 °C) on glass substrates. By controlling the concentration of the catalysts and the stamp printing conditions, we are able to fabricate

desired CNTs patterns with controlled 3D architectures. This catalyst system, together with the controlled fabrication of large area 3D patterns on glass substrates could be useful for device applications of multidimensional aligned CNTs.

References and Notes

(1) Sohn, J. I.; Lee, S.; Song, Y.; Choi, S.; Cho, K.; Nam, K. *Appl. Phys. Lett.* **2001**, *78*, 901.

(2) Fan, S.; Chapline, M.; Franklin, N.; Tombler, T.; Cassell, A.; Dai, H. *Science* **1999**, *283*, 512.

(3) (a) Yang, Y.; Huang, S.; He, H.; Mau, A. W. H.; Dai, L. *J. Am. Chem. Soc.* **1999**, *121*, 10832. (b) Huang, S.; Mau, A. W. H. *Appl. Phys. Lett.* **2003**, *82*, 697.

(4) Wei, B. Q.; Vajtai, R.; Jung, Y.; Ward, J.; Zhang, Y.; Ramanath, G.; Ajayan, P. M. *Nature* **2002**, *416*, 49516.

(5) (a) Kind, H.; Bonard, J.-M.; Emmenegger, C.; Nilsson, L. O.; Hernadi, K.; Maillard-Schaller, E.; Schlapbach, L.; Forro, L.; Kern, K. *Adv. Mater.* **1999**, *11*, 1285. (b) Kind, H.; Bonard, J.-M.; Forró, L.; Kern, K.; Hernadi, K.; Nilsson L.; Schlapbach, L. *Langmuir* **2000**, *16*, 6877.

(6) (a) Cassell, A. M.; Verma, S., Delzeit, L.; Meyyappan M.; Han, J. *Langmuir* **2001**, *17*, 260. (b) Cassell, A. M.; Franklin, N. R.; Tombler, T. W.; Chan, E. M.; Han J.; Dai, H. *J. Am. Chem. Soc.* **1999**, *121*, 7975. (c) Gu G.; Philipp, G.; Wu, X.; Burghard, M.; Bittner, A. M.; Roth, S. *Adv. Functional Mater.* **2001**, *11*, 295.

(7) Huang, S.; Mau, A. W. H.; Turney, T. W.; White, P. A.; Dai, L. *J. Phys. Chem. B* **2000**, *104*, 2193.

(8) Burghard, D.; Duesberg, G.; Philipp, G.; Muster, J.; Roth, S. *Adv. Mater.* **1998**, *10*, 584.

(9) (a) Chen, Q.; Dai, L. *J. Nanosci. Nanotechnol.* **2001**, *1*, 43. (b) Huang, S.; Dai, L. *J. Nanoparticle Res.* **2002**, *4*, 145. (c) Huang, S. *Chem. Phys. Lett.* **2003**, *374*, 157.

(10) Wang, X. B.; Liu, Y. Q.; Zhu, D. B. *Adv. Mater.* **2002**, *14*, 165.

(11) (a) Ren, Z. F.; Huang, Z. P.; Xu, J. H.; Wang, P. B.; Siegal, M. P.; Provencio, P. N. *Science* **1998**, *282*, 1105. (b) Ren, Z. F.; Huang, Z. P.; Wang, D. Z.; Wen, Z. J.; Xu, J. W.; Wang, J. H.; Calvet, L. E.; Chen, J.; Klemic, J. F.; Reed, M. A. *Appl. Phys. Lett.* **1999**, *75*, 1086.

(12) Jiang, Y.; Wu, Y.; Zhang, S.; Xu, C.; Yu, W.; Xie, Y.; Qian, Y. *J. Am. Chem. Soc.* **2000**, *122*, 12383.

(13) Li, Y. J.; Sun, Z.; Lau, S. P.; Chen, G. Y.; Tay, B. K. *Appl. Phys. Lett.* **2001**, *79*, 1670.

(14) Huang, S.; Dai, L.; Mau, A. W. H. *Adv. Mater.* **2002**, *14*, 1140.

(15) Owens, W. T.; Rodriguez, N. M. and Baker, R. T. K. *J. Phys. Chem.* **1992**, *96*, 5048.

(16) Baker R. T. K. and Waite, R. J. *J. Catal.* **1975**, *37*, 101.

(17) Kovalchuk, V. I.; Kuznetsov, B. N. *J. Mol. Catal. A: Chem.* **1995**, *102*, 103.

(18) Englisch, M.; Ranade, V. S.; Lercher, J. A. *J. Mol. Catal. A: Chem.* **1997**, *121*, 69.

(19) Rachmady, W.; Vannice, M. A. *J. Catal.* **2002**, *209*, 87.